Atmos. Chem. Phys. Discuss., 9, 13439–13474, 2009
www.atmos-chem-phys-discuss.net/9/13439/2009/

Atmospheric
Chemistry
and Physics
Discussions

This discussion paper is/has been under review for the journal *Atmospheric Chemistry and Physics (ACP)*. Please refer to the corresponding final paper in *ACP* if available.

Chemical apportionment of southern African aerosol mass and optical depth

B. I. Magi

Princeton University, Princeton, New Jersey, USA

Received: 7 June 2009 – Accepted: 8 June 2009 – Published: 18 June 2009

Correspondence to: B. I. Magi (brian.magi@noaa.gov)

Published by Copernicus Publications on behalf of the European Geosciences Union.

Abstract

We investigate the aerosol mass apportionment and derive aerosol optical properties that characterize the aerosol over extratropical and tropical southern Africa during the biomass burning season. We find that 54% and 83% of the extratropical and tropical aerosol mass, respectively, is composed of carbonaceous species, consistent with the fact that the major source of particulate matter in southern Africa is biomass burning. This mass apportionment implies that carbonaceous species in the form of organic carbon (OC) and black carbon (BC) play a critical role in the aerosol optical properties. By combining the in situ measurements of aerosol mass concentrations with concurrent measurements of aerosol optical properties at a wavelength of 550 nm, we find that 80–90% of the aerosol scattering is due to carbonaceous aerosol, where our derived mass scattering cross sections (MSC) for OC and BC are 3.9±0.6 m^2/g and 1.6±0.2 m^2/g, respectively. Our derived values of mass absorption cross sections (MAC) for OC and BC are 0.7±0.6 m^2/g and 8.2±1.1 m^2/g, respectively. The values of MAC imply that 26–27% of the aerosol absorption in southern Africa is due to OC, with the remainder due to BC. Our results provide important constraints for aerosol properties in a region dominated by biomass burning and should be integrated into climate models to improve aerosol simulations.

1 Introduction

Biomass burning is a major source of particulate matter in the atmosphere over Africa during the dry season. In southern Africa alone, biomass burning consistently accounts for 25% of the total number of fires that occur every year on the planet (Giglio et al., 2003, 2006), but in situ measurements of tropospheric aerosol mass concentrations in that region are rare. This was part of the motivation for the Southern African Research Initiative field campaign in August and September 2000 (SAFARI-2000), and resulted in a number of publications from about 2002 to present, many of which are summarized by Swap et al. (2003).

In this study, we synthesize in situ measurements of aerosol mass concentrations originally published in SAFARI-2000 studies by Eatough et al. (2003), Gao et al. (2003), and Kirchstetter et al. (2003). We do this to provide a measurement-based estimate of aerosol mass concentrations in a region of the world that is poorly simulated in most transport and circulation models (e.g. Ginoux et al., 2006; Kinne et al., 2006; Matichuk et al., 2007; Magi et al., 2009). The synthesis requires more than reviewing the research since there was a technical problem with part of the aerosol sampling system on the aircraft the bulk of this study is based on. This precluded the analysis of general regional haze properties for southern Africa until we were able to determine a solution to the problem, which we describe in Sect. 2. Our synthesis provides a mass apportionment of the southern African aerosol.

We then combine the aerosol mass concentrations with self-consistent aerosol optical properties discussed by Magi et al. (2008) to derive values of the mass scattering cross section (MSC) and the mass absorption cross sections (MAC) at a wavelength of 550 nm for measured aerosol species that are relevant to models. Using the derived MSC and MAC, we apportion the total scattering and absorption of the southern African aerosol. We discuss our methods to overcome the technical problem in Sect. 2, present the results in Sect. 3, offer an analysis in Sect. 4, and summarize our conclusions in Sect. 5.

2 Methods

2.1 Background

Gao et al. (2003) and Kirchstetter et al. (2003) discussed the methods of data collection and analysis, but we briefly reiterate what they said here. The teflon filter samples described by Gao et al. (2003) and the quartz filter samples described by Kirchstetter et al. (2003) (hereafter, referred to as G2003 and K2003, respectively) were usually collected in tandem on a manifold that pulled air through an inlet from outside the aircraft, across the filters, and exited the aircraft through an outlet. The inlet had a 2–3 µm particle diameter cut-off such that all reported results apply to $PM_{2.5}$ (i.e. particulate matter, PM, with diameters less than 2.5 µm). Teflon filter samples were analyzed for $PM_{2.5}$ aerosol mass concentration, and the mass concentrations of $PM_{2.5}$ ionic species like sulfate (SO_4^{2-}) and nitrate (NO_3^-), among others (see G2003). For simplicity in this study, we refer to the ionic species as SO_4 and NO_3. Quartz filter samples were analyzed for $PM_{2.5}$ carbonaceous aerosol mass concentration (see K2003), which was usually apportioned into organic carbon (OC) and black carbon (BC) components. Independent in situ evidence shows that the southern African aerosol in the polluted layer (below about 5 km) is dominated by particles with diameters less than 1.0 µm (Li et al., 2003; Posfai et al., 2003; Formenti et al., 2003).

The sampling system used to determine aerosol mass concentrations reported by Eatough et al. (2003) (hereafter, referred to as E2003) was completely independent of the manifold used to collect samples described by G2003 and K2003, but both sampling systems were on the same aircraft (see Appendix in Sinha et al., 2003). E2003 reported mass concentrations of OC, BC, SO_4, NO_3, and semi-volatile organic carbon (SVOC), noting that no other study has reported SVOC in southern Africa. SVOC is generally thought to be lost during in situ sampling and OC and BC (as reported by E2003 and K2003) does not include this additional mass.

Samples reported by E2003 were collected at a lower frequency than samples discussed by G2003 and K2003, but on average the samples all characterized the same aerosol. In Fig. 1, we show the locations of samples discussed by E2003, G2003, and K2003. Formenti et al. (2003) discussed samples collected during SAFARI-2000, but further west of the major burning regions. Ground-based results reported by Piketh et al. (1999) and Maenhaut et al. (1996) were collected in southern to eastern South Africa, but we restrict our analysis to aerosol samples collected in the troposphere since ground-based filter data are not always representative of the aerosol characteristics aloft.

We partition results in this study into categories based on the parcel back-trajectory analysis described by Magi and Hobbs (2003). Namely, samples collected when back-trajectories were from the south or east are one category, while those collected when back-trajectories were from the north or west are a second category. The sample area roughly covers northeast South Africa, eastern Botswana, and southern Zambia (Fig. 1), and therefore parcels arriving from the south or east are extratropical (south of 22.5° S) in origin, while those from the north or west are tropical (north of 22.5° S) in origin. Therefore, we refer to samples as either characterizing the "extratropics" or "tropics" based on this discussion.

Since nearly all fires in southern Africa occur in the tropics (Fig. 1), we would expect differences in aerosol properties (such as chemical composition, size, or number concentration) between samples characteristic of the tropics and the extratropics. We summarize the evidence showing the aerosol characteristics in Table 1, where we list the median aerosol optical properties at a wavelength of 550 nm and median aerosol physical properties, along with the respective interquartile range. Aerosol optical depth (AOD) is one of the most commonly reported aerosol optical properties, and is calculated as the vertical integral of aerosol extinction (EXT) or retrieved from remote sensing measurements. EXT itself is the sum of aerosol scattering (SCA) and absorption (ABS), where EXT, SCA, and ABS are in units of m^{-1} or Mm^{-1}. Single scattering albedo (SSA) is defined as SCA/EXT and physically represents the probability that radiation incident on a particle is scattered rather than absorbed. These aerosol optical properties are discussed in many scientific studies, but a good reference for definitions is the textbook by Seinfeld and Pandis (2006).

The summary statistics in Table 1 are based on data discussed by Magi et al. (2008) and by Magi (2006). The tropical aerosol properties have significantly higher AOD and lower SSA. Most of this is due to the factor of two increase in accumulation mode particle concentration (N_2 in Table 1), and very little of the difference can be attributed to changes in the shape of the size distribution (α) or an increase in coarse mode particle volume concentration (C/F). Since relative humidity (RH) affects ambient aerosol properties by increasing the size of the particles, which subsequently increases the AOD (e.g. Hegg et al., 1993), we list the median RH in Table 1 as well. Magi and Hobbs (2003) showed that aerosol scattering coefficients in southern Africa are not significantly affected when RH is less than ~50%, so it is clear from Table 1 that the very dry conditions eliminated the possibility that RH could explain the AOD differences in the tropics and extratropics. In the next section, we discuss the results of the filter samples with respect to these aerosol properties.

2.2 Miscalibrated flow meters

Mass concentrations derived from filters depends on the total flow (m^3) that passes across the filters. The three flow meters used to measure the flows for G2003 and K2003 were calibrated against a bubble flow meter before and after the SAFARI-2000 campaign and compared to a separate flow meter on the aircraft during the campaign. Each flow meter had a different set of calibration coefficients. In all cases, total flow was reported at standard temperature and pressure (STP) so that mass concentrations derived at different atmospheric levels could be directly compared.

After the SAFARI-2000 campaign, we realized that the calibration coefficients of the flow meters were dependent on whether multiple flow meters were in use. The end result was that the total flows measured by the flow meters used for the filters reported by G2003 were in error by some unknown value. The flow meter used with the filters reported by K2003 were not affected because of the position of the flow meter on the aircraft manifold. We were able to verify this qualitatively (simple observations during the campaign), but the flow meters were removed from the manifold before we could quantitatively verify the calibration coefficients for the flow meters used for filters described by G2003. Therefore, although we had tandem filter samples, absolute comparisons between results by G2003 and by K2003 were not possible since one of the filter measurements (usually the teflon filters) used a flow meter with an unknown calibration constant.

As evidence of the problem introduced by the defective flow meter, we summarize mass concentrations reported by G2003, K2003, and E2003 in Table 2. OC and BC reported by K2003 generally agreed with results by E2003 to within the bounds of the interquartile range or within the ∼30% measurement uncertainty. The agreement is better in the extratropics (Table 2a) than in the tropics (Table 2b), but this could be because the sample size of E2003 filters representative of the tropics is only four. However, results by G2003 (measured at the same time as K2003) do not agree with the results by E2003 (referring to $PM_{2.5}$, SO_4, and NO_3 in Table 2). The discrepancy is most clear when we examine the ratio of aerosol mass concentrations from the tropics to the extratropics. G2003 results suggest a tropics to extratropics $PM_{2.5}$ ratio of 0.8, while E2003 results suggest a ratio of 3.1. The corresponding ratio of OC for K2003 3.5, while for E2003 is 5.8. Thus, G2003 data suggests that $PM_{2.5}$ decreases in the tropics, while E2003 suggests an increase. Yet, OC reported by K2003 and E2003 clearly increases in the tropics due to more widespread burning (Fig. 1). Table 1 provides further evidence of the discrepancy by showing a significant increase in AOD and accumulation mode aerosol number concentrations (Sect. 2.1) with no evidence supporting a significant change in the dominant particle size of the aerosol size distribution (i.e. C/F and α in Table 1). The major reason for the difference in AOD in the samples is thus due to an increase in aerosol number concentration, and therefore we expect an increase in $PM_{2.5}$ mass. G2003 results in Table 2 contradict this evidence, while E2003 and K2003 support the evidence.

2.3 Proxy calibration

In order to partition the aerosol mass or make any generalizations about measured aerosol mass, absolute mass concentrations must be used. We developed a working solution to overcome the problem of miscalibrated flow meters based on three separate pieces of information: 1. We knew which flow meters were used to measure flow for each sample, 2. On four occasions we collected duplicate samples by sampling aerosol on pairs of the same type of filters (twice with teflon, twice with quartz) and monitoring the flow rate through each filter using different flow meters, and 3. The independent sampling system (and flow meter) described by E2003 was on the same aircraft.

The most important information helping us formulate a working solution were the simultaneous filter samples, which we assumed should report nearly identical mass concentrations. The intended purpose of the simultaneous filter samples was to characterize the noise inherent in the measurements of filter mass for the technique described by G2003 and by K2003, but they resulted in a convenient solution to the miscalibrated flow meter. We list the results of the simultaneous filter samples in Table 3 as Test 1 and Test 2 (obtained on two different days), and it is clear that there are discrepancies well beyond the expected noise in reported mass concentration. Namely, the Test 1 results from "Flow 1" for teflon filters ($PM_{2.5}$, NO_3, SO_4) and for quartz filters (OC, BC) should be roughly the same as the results from "Flow 2". Similarly, Test 2 results from "Flow 2" and "Flow 3" should be roughly the same as well. Generally, Flow 2 was used to derive measurements reported by K2003, while Flow 1 and Flow 3 were used to derived measurements from the teflon filters.

Purely by coincidence, the teflon filters obtained from the tropics were derived using Flow 1 while the extratropical samples were obtained using Flow 3. All quartz filters were obtained using Flow 2, which was correctly calibrated (i.e. unaffected when multiple flow meters were in use). Using Table 3, the median ratio of mass concentrations reported by Flow 2 to mass concentrations reported by Flow 1 was 3.4 (interquartile range of 3.1 to 4.3), while the ratio of Flow 2 to Flow 3 was 0.45 (0.44 to 0.45). Assuming the mass (in µg) reported in Table 3 should be equal, the fact that the ratios were greater than or less than unity is due entirely to difference in the flow (in m^3) and we can use this as a proxy for direct calibration.

Evidence supporting this proxy calibration using Table 3 comes from the third piece of information. We can ratio $PM_{2.5}$ reported in Table 2 for the tropics from E2003 to $PM_{2.5}$ reported by G2003 for the tropics, which, because all the teflon filter samples from the tropics were collected using Flow 1, should be similar to the ratio of Flow 2 to Flow 1 (stated above as 3.4). The ratio of E2003 to teflon filter samples in the tropics is 3.8 (interquartile range of 3.2 to 6.1), which encompasses the median value of 3.4

reported above. The ratio in the extratropics is 0.55 (0.52 to 0.68), which is greater than the median value of 0.45, but roughly similar.

Using the information described above as a proxy for calibration coefficients for the miscalibrated flow meters (i.e. Flow 1 and Flow 3), we corrected the mass concentrations derived from the teflon filters. We list the statistics from the corrected mass concentrations in Table 4, noting that values of OC and BC are nearly identical to those listed in Table 2 since the carbon aerosol mass concentrations were mainly derived using the properly calibrated flow meter (Flow 2). $PM_{2.5}$, SO_4, and NO_3 are all different than the values in Table 2, and with the exception of SO_4 in the tropics, the interquartile ranges of all mass concentrations now overlap with the mass concentrations derived from E2003. Considering that the teflon and quartz filters were collected at different times than the samples reported by E2003, the agreement is quite good. The only reason we expect any agreement at all is that E2003 was on the same aircraft and very generally sampled the same atmospheric haze sampled by teflon and quartz filter samples. Thus, we conclude that after applying the proxy calibration of flow meters used to derive mass concentrations from teflon filters, the mass concentrations derived from teflon and quartz filter samples can now be analyzed together with those reported by E2003. These corrected mass concentrations are what we refer to in the next sections and in our conclusions.

3 Results

3.1 $PM_{2.5}$ aerosol mass

The statistics of the speciated mass concentrations from all the filter samples (teflon, quartz, and those reported by E2003) are listed in Table 5. $PM_{2.5}$ mass concentrations are about 12 µg/m^3 in the extratropics and increase by a factor of four in the tropics to nearly 48 µg/m^3. This increase is consistent with the data in Fig. 1 which shows that the tropics are where most burning occurs every year and with aerosol physical and optical properties listed in Table 1. The speciated mass apportionment reveals that the primary driving force for the increase in $PM_{2.5}$ is an increase in OC and BC mass. NO_3 mass increases by a factor of 14 to a concentration of about 2.6 µg/m^3. Although this NO_3 mass concentration is greater than typical background concentrations reported by Sinha et al. (2003) and Tripathi et al. (1996), NO_3 still accounts for less than 5% of the $PM_{2.5}$ mass.

Both SO_4 and SVOC aerosol mass concentrations in Table 5 are not significantly different in the tropics compared to the extratropics. The lack of difference in SO_4 could partly be attributed to additional SO_4 sources in the extratropics that are not biomass burning in origin (Piketh et al., 1999; Bond et al., 2007). SVOC mass statistics are based on ten samples in the extratropics and four samples in the tropics, so the limited sample sizes may not be sufficient to support any conclusion about SVOC in the tropics versus the extratropics. The interquartile range of SVOC, for example, is much larger in the tropics, presumably indicating that the fire and/or biomass characteristics also were different among the four samples.

3.2 $PM_{2.5}$ mass apportionment

Using the information in Table 5, and converting the measured species to common molecular forms, we can apportion the $PM_{2.5}$ aerosol mass. We convert the ionic aerosol species (SO_4 and NO_3) to ammonium sulfate ($(NH_4)_2SO_4$) and ammonium nitrate (NH_4NO_3) by multiplying the mass of SO_4 and NO_3 by 1.38 and 1.29, respectively. Conversion of OC to organic matter (OM) to account for the non-carbon mass of molecular forms of OC is subject to considerable uncertainty. Dentener et al. (2006) suggest a conversion factor of 1.4. Turpin and Lim (2001) suggest that 1.4 should be considered a lower bound to estimates and that a value of 1.6±0.2 and 2.1±0.2 are more representative of urban and non-urban aerosols, respectively, but they point out that even this range is subject to re-examination considering how little we still understand about the many compounds that together comprise "OC" (e.g. Kanakidou et al., 2005). We derive a OM/OC ratio for the extratropics and tropics by assuming that we can account for 100% of the $PM_{2.5}$ mass with NH_4NO_3, $(NH_4)_2SO_4$, BC, and OM (including SVOC makes no difference in this case). Thus, $OM/OC=(PM_{2.5}-NH_4NO_3-(NH_4)_2SO_4-BC)/OC$. This gives a value of 1.4 (interquartile range is 1.0 to 1.6) for OM/OC in the extratropics and 2.1 (1.6 to 3.0) for OM/OC in the tropics. The median values we derived are within the broad range of 1.4–2.3 suggested above.

In Fig. 2, we show the chemical apportionment of $PM_{2.5}$ mass. In the extratropics, 54% of the aerosol mass is OM and BC, while the remaining 46% is comprised of NH_4NO_3 and $(NH_4)_2SO_4$. As discussed above, $(NH_4)_2SO_4$ is roughly the same in the tropics and the extratropics, but the dramatic increase in OM and BC in the tropics results in an aerosol comprised of 83% carbonaceous components. If we include SVOC, the contribution of carbonaceous particles to $PM_{2.5}$ mass increases to 69% in the extratropics and 85% in the tropics.

3.3 Aerosol optical depth apportionment

In this Section, we describe the apportionment of AOD at a wavelength of 550 nm. Most of the speciated aerosol mass concentrations that comprise the median values listed in Table 5 were coincident with measurements of SCA and ABS (with a $PM_{2.5}$ aerosol cut-off) at a "dry" relative humidity (RH) of 30% (see Magi et al., 2003, 2008 for details about the measurements of SCA and ABS). We report aerosol mass concentrations in this study at standard temperature and pressure (STP) and for dry aerosol mass, so we also adjust the dry SCA and ABS to STP. Thus, we can relate the species mass concentrations to SCA and ABS by assuming that each species plays independent roles in determining the totals by

$$\mathrm{SCA} = \sum_{i=1}^{4} M_i \times \mathrm{MSC}_i \qquad (1a)$$

$$\mathrm{ABS} = \sum_{i=1}^{4} M_i \times \mathrm{MAC}_i \tag{1b}$$

where M_i is the mass concentration of NH_4NO_3, $(NH_4)_2SO_4$, OM, and BC and MSC_i and MAC_i are the mass scattering and mass absorption cross sections (e.g. Bond and Bergstrom, 2006), in units of m^2/g. SCA and ABS in these equations and those that follow are at a dry RH and at STP.

All the aerosol species contribute to scattering. For the multiple linear regression, we combine the mass concentrations of NH_4NO_3 and $(NH_4)_2SO_4$ together and OM and BC together, such that we modify Eq. (1a) to be

$$\mathrm{SCA} = M_{\mathrm{ionic}} \times \mathrm{MSC}_{\mathrm{ionic}} + M_{\mathrm{carbon}} \times \mathrm{MSC}_{\mathrm{carbon}} \tag{2}$$

where M_{ionic} is the sum of NH_4NO_3 and $(NH_4)_2SO_4$ and M_{carbon} is the sum of OM and BC. The regression is unstable if we separately consider the four aerosol species, mainly due to the relatively small sample size. Since we attempt to attribute all the scattering to these aerosol species, it is also important to consider the molecular forms of the species (i.e. NH_4NO_3, $(NH_4)_2SO_4$, and OM as opposed to NO_3, SO_4, and OC). We then partition the values of M_{ionic} and M_{carbon} using Mie theory approximations to derive $\mathrm{MSC}_{\mathrm{OC}}$, $\mathrm{MSC}_{\mathrm{BC}}$, $\mathrm{MSC}_{\mathrm{SO_4}}$, and $\mathrm{MSC}_{\mathrm{NO_3}}$.

We simplify Eq. (1b) since we know a priori that NH_4NO_3 and $(NH_4)_2SO_4$ do not significantly absorb visible radiation (e.g. Tang and Munkelwitz, 1994) while BC and OC are both potential absorbers (e.g. Bond and Bergstrom, 2006; Kirchstetter et al., 2004). Therefore Eq. (1b) becomes

$$\mathrm{ABS} = M_{\mathrm{OC}} \times \mathrm{MAC}_{\mathrm{OC}} + M_{\mathrm{BC}} \times \mathrm{MAC}_{\mathrm{BC}} \tag{3}$$

noting that BC is the major absorbing aerosol species in the mid-visible, while OC absorption seems to vary depending on the location. Kirchstetter et al. (2004) showed that OC accounts for about 7–24% of the total absorption at a wavelength of 550 nm, with an imaginary refractive index of about 0.03. Kanakidou et al. (2005) summarize research about OC and suggest an imaginary refractive index for OC of about 0.006. Transport models discussed by Kinne et al. (2006) assumed an imaginary refractive index of 0.03, similar to findings discussed by Kirchstetter et al. (2004). Even a very small OC contribution to total absorption is important, however, since OC mass burden is often much greater than BC mass burden (e.g. Bond et al., 2004).

We use multiple linear regression to solve Eqs. (2) and (3) for MSC and MAC and list the values (at 550 nm) in Table 6 along with the standard errors. We also list MSC and MAC calculated from Mie theory in Table 6, where the assumptions we used to calculate the theoretical MSC and MAC are listed in Table 7 (lognormal size distribution diameter and standard deviation, density, and refractive indices at 550 nm). The values in Table 7 for OC are similar to those used in models (e.g. Kinne et al., 2006) and suggested in the review study by Kanakidou et al. (2005), while the density of OC is based on discussions by Turpin and Lim (2001). The values for BC are based on discussions by Kirchstetter et al. (2004) and by the analysis by Bond and Bergstrom (2006). The values we used to simulate NH_4NO_3 and $(NH_4)_2SO_4$ are based on Tang and Munkelwitz (1994).

We derive values of MSC_{OC}, MSC_{BC}, MSC_{SO_4}, and MSC_{NO_3} by partitioning the values of MSC_{ionic} and MSC_{carbon} from Eq. (2) according to the theoretical contributions predicted by Mie theory. Thus $MSC_{SO_4}=0.47\times1.38\times MSC_{ionic}$ and $MSC_{NO_3}=0.53\times1.29\times MSC_{ionic}$, where the 0.47 and 0.53 are the fractional contributions to MSC_{ionic} and 1.38 and 1.29 are the molecular conversion factors. For MSC_{carbon}, we derive $MSC_{OC}=0.59\times1.7\times MSC_{carbon}$ and $MSC_{BC}=0.41\times MSC_{carbon}$, where 0.59 and 0.41 are the fractional contributions to MSC_{carbon} and 1.7 is the mean ratio of OM to OC. In all cases, using literature-based assumptions to simulate the aerosol components, we can match the measurement-based MSC and MAC with theoretical values of MSC and MAC. We analyze these results in the next Section.

4 Analysis

4.1 Aerosol mass

The evidence we presented clearly shows that the more intense burning in tropical southern Africa results in an aerosol that is significantly different than extratropical southern Africa. These differences apply to aerosol optical properties and number concentrations (Table 1), $PM_{2.5}$ mass concentrations (Table 5), and even $PM_{2.5}$ mass apportionment (Fig. 2). The major differences are that tropical southern African aerosol is composed of 83% carbonaceous aerosol, while the extratropical southern African aerosol is composed of 54% carbonaceous aerosol and $PM_{2.5}$ mass increases by a factor of four in the tropical aerosol due mainly to increases in OC mass. The extratropical aerosol samples we discuss in this study are most likely biased towards the more intense biomass burning since the sample locations (Fig. 1) are located east of the Namib and Kalahari deserts. Although we did not confirm this, sulfate aerosol contributions from industrial sources in northeast South Africa (e.g. Bond et al., 2007; Piketh et al., 1999) may also affect the mass apportionment we showed in Fig. 2a. The fractional contributions to overall $PM_{2.5}$ mass that we derived from measurements should be considered when simulating the aerosol over southern Africa.

Formenti et al. (2003) characterized southern African aerosol properties near Namibia (15–25° S, 10–15° E) during SAFARI-2000. If we consider their reported values of mass concentrations of NH_4NO_3, $(NH_4)_2SO_4$, OM, and BC, then carbonaceous aerosol makes up about 70–90% of $PM_{2.5}$ mass. Even considering all of the reported species in Formenti et al. (2003), $PM_{2.5}$ aerosol is composed of about 60–75% carbonaceous aerosol. Although the samples discussed by Formenti et al. (2003) are west and south of major burning regions, particles emitted from biomass burning are often transported from both tropical and extratropical burning regions over Namibia and over the southeast Atlantic Ocean (e.g. Garstang et al., 1996). Formenti et al. (2003) also confirmed this transport pathway with an analysis of back-trajectories of their sample locations. The mass concentrations of NO_3, SO_4, OC, and BC reported by Formenti et al. (2003) range from 1.0–1.4, 1.9–2.0, 6–20, and 1.0–2.0 µg/m^3, respectively. Compared to values in Table 5, our measurements of NO_3, OC, and BC are all very similar, while we report a factor of two higher SO_4 mass concentration. The higher SO_4 concentration is expected since many of our samples were affected by proximity to intense burning (tropics) or proximity to industrial sources (extratropics).

Ruellan et al. (1999) collected aircraft-based in situ aerosol samples during the Experiment for Regional Sources and Sinks of Oxidants (EXPRESSO) field campaign in November and December 1996 over Northern Hemisphere equatorial Africa (3–5° N, 17–19° E). Fires in this region in November and December are as numerous as those in tropical southern Africa during August and September, so we would expect some similarities in the aerosol regardless of the differences in burning characteristics (i.e. vegetation, combustion completeness). Ruellan et al. (1999) reported mean OC and BC mass concentrations of about 22±11 and 5±2 µg/m^3, respectively, between the surface and about 4 km. This is very similar to median OC and BC mass concentrations we report for tropical southern Africa in Table 5 of 17 µg/m^3 (12–23 µg/m^3 interquartile range) and 3.4 µg/m^3 (1.8–4.5 µg/m^3 interquartile range), respectively.

Across the entire African region, there is variability in aerosol mass concentration in the polluted layer, but the magnitudes generally agree in terms of carbonaceous aerosol. Based on a small number of studies from EXPRESSO and SAFARI-2000, the carbonaceous aerosol mass concentration seems to decrease from north to south and from east to west. This is consistent with fire occurrence patterns derived from MODIS (Giglio et al., 2003; 2006). Both this study, which is based on data originally described by E2003, G2003, and K2003, and the study by Formenti et al. (2003), suggest that at least half the $PM_{2.5}$ aerosol mass concentration during the biomass burning season is composed of carbonaceous aerosol. This fraction increases significantly as $PM_{2.5}$ mass increases.

In Fig. 3, we show the correlation of OC, BC, NO_3, and SO_4 mass with $PM_{2.5}$ mass and, with the exception of SO_4, all are significantly correlated (p-values less than 0.05, implying the correlation is significant with greater than 95% confidence). OC is clearly the main factor driving increases in $PM_{2.5}$ mass, with r^2=0.93. SO_4 on the other hand is not significantly correlated, and only about 27% of the variance in $PM_{2.5}$ can be explained by SO_4.

The significant correlations of OC and BC mass with $PM_{2.5}$ mass is not restricted to the tropics or the extratropics. The correlation of NO_3 and SO_4 with $PM_{2.5}$, however, does depend on the regional subset. Namely, SO_4 is significantly correlated with $PM_{2.5}$ in the extratropics (r^2=0.82), and NO_3 is significantly correlated with $PM_{2.5}$ in the tropics (r^2=0.78), while the opposite in both cases is not true. The better correlation of NO_3 with $PM_{2.5}$ in the tropics where burning is more prevalent agrees with results discussed by Hobbs et al. (2003) which suggested NO_3 enhancements in aged smoke due to secondary (photochemical) formation. We suggest that the major SO_4 sources in the extratropics are split between biomass burning and fossil fuel burning in northeastern South Africa and that this explains why SO_4 is better correlated with $PM_{2.5}$ in the extratropics than the tropics.

4.2 Mass scattering and mass absorption cross sections

The unifying characteristics of the tropical and extratropical southern Africa aerosol are the values of MSC and MAC, especially with respect to carbon species (OC and BC). Using the multiple linear regression technique described in Sect. 3.3, $MSC_{OC}=3.9\pm0.6\,m^2/g$ and $MSC_{BC}=1.6\pm0.2\,m^2/g$ (Table 6). Based on previous work, we assumed all the absorption was due to OC and BC and showed that $MAC_{OC}=0.7\pm0.6\,m^2/g$ and $MAC_{BC}=8.2\pm1.1\,m^2/g$ (Table 6). MSC_{SO_4} and MSC_{NO_3} are both very small and the uncertainty in the multiple linear regression coefficients is large. All of our measurement-based results, however, are consistent with Mie theory, although we point out that the theoretical values are dependent on assumptions listed in Table 7.

In a detailed review of past research related to BC absorption and a critical analysis of BC absorption by Bond and Bergstrom (2006), they suggested that MSC_{BC} varied from about 1.6 to 3.7 m^2/g and $MAC_{BC}=7.5\pm1.2\ m^2/g$. Our values of MSC_{BC} and MAC_{BC} in Table 6 agree to within uncertainty with Bond and Bergstrom (2006). OC optical properties, particularly absorption, are a much more poorly understood aspect of aerosol science. Kirchstetter et al. (2004) derived a value of $MAC_{OC}=0.6\ m^2/g$ from smoke samples collected during SAFARI-2000, while Sun et al. (2007) suggest $MAC_{OC}=1.0\ m^2/g$ based on a theoretical model of a combustion aerosol. Our value of $0.7\pm0.6\ m^2/g$ agrees well with these past studies, especially considering the much different methodologies. Our value of MSC_{OC} is on the high end of previously published values of MSC_{OC}, which range from 1–5 m^2/g and are sometimes based on data, and sometimes based on assumptions (e.g. White, 1990; Liousse et al., 1996; Magi et al., 2009).

The single scattering albedo (SSA) at 550 nm is defined as MSC/MEC where MEC is the mass extinction cross section and is the sum of MSC and MAC. MSC/MEC and SCA/EXT as described in Sect. 2.1 are equivalent ways of calculating SSA. SSA_{SO_4} and SSA_{NO_3} are therefore equal to 1 due to our assumptions, but $SSA_{OC}=0.85$ and $SSA_{BC}=0.17$. Bond and Bergstrom (2006) suggest that $SSA_{BC}=0.2$–0.3, so our derived values fall on the low end of that range. In a modeling study, Magi et al. (2009) suggested $SSA_{OC}=0.97$ and $SSA_{BC}=0.21$, but also showed that the overall aerosol SSA simulated by the model was biased high compared to measurements. We suggest that high biases in modeled SSA (e.g. Kinne et al., 2006) would improve if models simulated a more strongly absorbing OC component in regions of the world impacted by biomass burning, as our data suggests.

4.3 Apportionment of scattering and absorption

Using the MSC and MAC we derived from multiple linear regression, we apportion the scattering and absorption in the extratropics and the tropics. In the apportionment, we revert to the molecular forms of the species for scattering since all the aerosol mass is responsible for scattering solar radiation. We refer to OC and BC for absorption since there is no evidence suggesting the additional mass in OM (as opposed to OC) is absorbing.

The results of aerosol optical properties apportionment for the extratropics are shown in Fig. 4 while the tropical apportionment is shown in Fig. 5. Both figures reveal similar trends, but NH_4NO_3 and $(NH_4)_2SO_4$ account for about twice the scattering in the extratropics than in the tropics. Carbonaceous aerosol accounts for an overwhelming 80–90% of the total scattering.

The evidence we present in Figs. 4b and 5b suggests that OC accounts for about 26–27% of the absorption, while BC accounts for the remainder. These numbers agree with SAFARI-2000 results by Kirchstetter et al. (2004), who used a much different methodology and showed that OC accounts for 7–24% of the absorption at 550 nm for freshly emitted smoke. Although the differences between Kirchstetter et al. (2004) and this study are not statistically significant, the generally higher contribution of OC to absorption in this study might be due to enhanced OC absorption from secondary particle formation as the plume smoke ages in the atmosphere. In terms of the scales involved in simulating an aerosol in climate models, it is perhaps more appropriate to model the properties of an aged aerosol.

5 Conclusions

Using synthesized results from three previously published studies, we characterized the southern African aerosol during the biomass burning season, which occurs consistently from May to October. Our synthesis provided speciated aerosol mass that we argued was representative of tropical and extratropical southern Africa. $PM_{2.5}$ mass in the tropics is about a factor of four greater than in the extratropics (Table 5), and this is driven primarily by increases in carbonaceous aerosol mass from the more widespread occurrence of fires in the tropics. The magnitude and species contributions to total aerosol mass in this study (Fig. 2), after applying corrections described in Sect. 2, agree well with other studies of African aerosols dominated by biomass burning (Ruellan et al., 1999; Formenti et al., 2003). We used the aerosol mass concentrations together with measurements of aerosol optical properties (Magi et al., 2008) to derive mass scattering cross sections (MSC) and mass absorption cross sections (MAC) for the aerosol species. Our measurement-based MSC and MAC for carbonaceous aerosol species (Table 6) all agreed with theoretical values of MSC and MAC predicted by Mie theory and with literature-based values.

The results presented in this study support the theory that the organic carbon (OC) component of an aerosol dominated by biomass burning particles absorbs a significant fraction of visible radiation. Climate models rely on a variety of assumptions about the basic properties (size, composition, refractive index, mixing state) of black carbon (BC) that are inconsistent with recent research (Bond and Bergstrom, 2006), and recent results (e.g. Kirchstetter et al., 2004) suggest the same is true for OC. As we showed in this study, carbonaceous aerosol mass accounts for 54–83% of the aerosol mass over southern Africa, so assumptions about BC and OC are particularly important over biomass burning regions. Our results support the findings of Bond and Bergstrom (2006) regarding BC and those by Kirchstetter et al. (2004) for OC.

Wild (2008) points out that climate models contributing to the IPCC 4th Assessment Report do not adequately account for absorbing aerosol, and most (see Meehl et al., 2007) do not even include OC and BC as forcing agents in climate simulations. Of the IPCC models that do include OC and BC, only the NASA GISS model (Liu et al., 2006) uses a treatment of OC absorption that is consistent with results by Kirchstetter et al. (2004). Both the NOAA GFDL (Magi et al., 2009) and the MPI ECHAM5-HAM (Stier et al., 2005) models use imaginary refractive indices for OC that are about five times less than suggested by current measurement-based results (Kirchstetter et al., 2004). The implications of more strongly absorbing OC on global and regional climate needs to be investigated, but as Wild (2008) showed, it is clear that the surface radiation budget cannot be properly simulated until we better understand basic aerosol properties and assimilate this understanding into climate models.

Models need to examine both the assumed properties of carbonaceous aerosol species and the subsequent mass apportionment in biomass burning regions to fully understand any discrepancies (e.g. Liu et al., 2006; Magi et al., 2009) that may exist. Our results will improve the understanding of both of these issues. In future work, we will discuss the wavelength dependence of the mass scattering and mass absorption cross sections over southern Africa for the major aerosol species simulated in climate models. This will provide further constraint on assumptions required by models to simulate the biomass burning component of the global aerosol.

Acknowledgements. We thank Delbert Eatough, Song Gao, and Tom Kirchstetter for the data discussed in this study. We thank Tom Kirchstetter and Song Gao for offering useful comments on a draft of this paper. Finally, we thank Tami Bond and Christian Metzler for writing a very useful Matlab version of the Bohren and Huffman Mie code and making it available at http://www.hiwater.org.

References

Bond, T. C., Streets, D. G., Yarber, K. F., Nelson, S. M., Woo, J., and Klimont, Z.: A technology-based global inventory of black and organic carbon emissions from combustion, J. Geophys. Res., 109, D14203, doi:10.1029/2003JD003697, 2004.

Bond, T. C. and Bergstrom, R. W.: Light absorption by carbonaceous particles: an investigative review, Aerosol Sci. Tech., 40, 27–67, 2006.

Bond, T. C., Bhardwaj, E., Dong, R., Jogani, R., Jung, S., Roden, C., Streets, D. G., and Trautmann, N. M.: Historical emissions of black and organic carbon aerosol from energy-related combustion, 1850–2000, Global Biogeochem. Cy., 21, GB2018, doi:10.1029/2006GB002840, 2007.

Dentener, F., Kinne, S., Bond, T., Boucher, O., Cofala, J., Generoso, S., Ginoux, P., Gong, S., Hoelzemann, J. J., Ito, A., Marelli, L., Penner, J. E., Putaud, J.-P., Textor, C., Schulz, M., van der Werf, G. R., and Wilson, J.: Emissions of primary aerosol and precursor gases in the years 2000 and 1750 prescribed data-sets for AeroCom, Atmos. Chem. Phys., 6, 4321–4344, 2006,
http://www.atmos-chem-phys.net/6/4321/2006/.

Eatough, D. J., Eatough, N. L., Pang, Y., Sizemore, S., Kirchstetter, T. W., Novakov, T., and Hobbs, P. V., Semivolatile particulate organic material in southern Africa during SAFARI 2000, J. Geophys. Res., 108(D13), 8479, doi:10.1029/2002JD002296, 2003.

Formenti, P., Elbert, W., Maenhaut W., Haywood, J., Osborne, S., and Andreae, M. O.: Inorganic and carbonaceous aerosols during the Southern African Regional Science Initiative (SAFARI 2000) experiment: chemical characteristics, physical properties, and emission data for smoke from African biomass burning, J. Geophys. Res., 108(D13), 8488, doi:10.1029/2002JD002408, 2003.

Gao, S., Hegg, D. A., Hobbs, P. V., Kirchstetter, T. W., Magi, B. I., and Sadilek, M.: Water-soluble organic components in aerosols associated with savanna fires in southern Africa: identification, evolution, and distribution, J. Geophys. Res., 108(D13), 8491, doi:10.1029/2002JD002324, 2003.

Garstang, M., Tyson, P. D., Swap, R., Edwards, M., Kallberg, P., and Lindesay, J. A.: Horizontal and vertical transport of air over southern Africa, J. Geophys. Res., 101(D19), 23721–23736, 1996.

Giglio, L., Descloitres, J., Justice, C. O., and Kaufman, Y. J.: An enhanced contextual fire detection algorithm for MODIS, Remote Sens. Environ., 87(2–3), 273–282, 2003.

Giglio, L., van der Werf, G. R., Randerson, J. T., Collatz, G. J., and Kasibhatla, P.: Global estimation of burned area using MODIS active fire observations, Atmos. Chem. Phys., 6, 957–974, 2006,
http://www.atmos-chem-phys.net/6/957/2006/.

Ginoux, P., Horowitz, L. W., Ramaswamy, V., Geogdzhayev, I. V., Holben, B. N., Stenchikov, G., and Tie, X.: Evaluation of aerosol distribution and optical depth in the Geophysical Fluid Dynamics Laboratory coupled model CM2.1 for present climate, J. Geophys. Res., 111, D22210, doi:10.1029/2005JD006707, 2006.

Hegg, D. A., Larson, T., and Yuen, P. F.: A theoretical study of the effect of relative humidity on light scattering by tropospheric aerosols, J. Geophys. Res., 98, 18435–18439, 1993.

Hobbs, P. V., Sinha, P., Yokelson, R. J., Bertschi, I. T., Blake, D. R., Gao, S., Kirchstetter, T. W., Novakov, T., and Pilewskie, P.: Evolution of gases and particles from a savanna fire in South Africa, J. Geophys. Res., 108(D13), 8485, doi:10.1029/2002JD002352, 2003.

Kanakidou, M., Seinfeld, J. H., Pandis, S. N., Barnes, I., Dentener, F. J., Facchini, M. C., Van Dingenen, R., Ervens, B., Nenes, A., Nielsen, C. J., Swietlicki, E., Putaud, J. P., Balkanski, Y., Fuzzi, S., Horth, J., Moortgat, G. K., Winterhalter, R., Myhre, C. E. L., Tsigaridis, K., Vignati, E., Stephanou, E. G., and Wilson, J.: Organic aerosol and global climate modelling: a review, Atmos. Chem. Phys., 5, 1053–1123, 2005, http://www.atmos-chem-phys.net/5/1053/2005/.

Kinne, S., Schulz, M., Textor, C., Guibert, S., Balkanski, Y., Bauer, S. E., Berntsen, T., Berglen, T. F., Boucher, O., Chin, M., Collins, W., Dentener, F., Diehl, T., Easter, R., Feichter, J., Fillmore, D., Ghan, S., Ginoux, P., Gong, S., Grini, A., Hendricks, J., Herzog, M., Horowitz, L., Isaksen, I., Iversen, T., Kirkevåg, A., Kloster, S., Koch, D., Kristjansson, J. E., Krol, M., Lauer, A., Lamarque, J. F., Lesins, G., Liu, X., Lohmann, U., Montanaro, V., Myhre, G., Penner, J., Pitari, G., Reddy, S., Seland, O., Stier, P., Takemura, T., and Tie, X.: An AeroCom initial assessment –optical properties in aerosol component modules of global models, Atmos. Chem. Phys., 6, 1815–1834, 2006, http://www.atmos-chem-phys.net/6/1815/2006/.

Kirchstetter, T. W., Novakov, T., Hobbs, P. V., and Magi, B.: Airborne measurements of carbonaceous aerosols in southern Africa during the dry, biomass burning season. J. Geophys. Res., 108(D13), 8476, doi:10.1029/2002JD002171, 2003.

Kirchstetter, T. W., Novakov, T., and Hobbs, P. V.: Evidence that the spectral dependence of light absorption by aerosols is affected by organic carbon, J. Geophys. Res., 109(D21), D21208, doi:10.1029/2004JD004999, 2004.

Li, J., Posfai, M., Hobbs, P. V., and Buseck, P. R.: Individual aerosol particles from biomass burning in southern Africa: 2. Compositions and aging of inorganic particles, J. Geophys. Res., 108(D13), 8484, doi:10.1029/2002JD002310, 2003.

Liousse C., Penner, J. E., Chuang, C., Walton, J. J., Eddleman, H., and Cachier, H.: A global three-dimensional model study of carbonaceous aerosols, J. Geophys. Res., 101, 19411–19432, 1996.

Liu, L., Lacis, A. A., Carlson, B. E., Mishchenko, M. I., and Cairns, B.: Assessing Goddard Institute for Space Studies ModelE aerosol climatology using satellite and ground-based measurements: a comparison study, J. Geophys. Res., 111, D20212, doi:10.1029/2006JD007334, 2006.

Maenhaut, W., Salma, I., Cafmeyer, J., Annegarn, H. J., and Andreae, M. O.: Regional atmospheric aerosol composition and sources in the eastern Transvaal, South Africa, and impact of biomass burning, J. Geophys. Res., 101(D19), 23631–23650, 1996.

Magi, B. I. and Hobbs, P. V.: Effects of humidity on aerosols in southern Africa during the biomass burning season. J. Geophys. Res., 108(D13), 8495, doi:10.1029/2002JD002144, 2003.

Magi, B. I., Hobbs, P. V., Schmid, B., and Redemann, J.: Vertical profiles of light scattering, light absorption and single-scattering albedo during the dry, biomass burning season in southern Africa and comparisons of in-situ and remote sensing measurements of aerosol optical depth, J. Geophys. Res., 108(D13), 8504, doi:10.1029/2002JD002361, 2003.

Magi, B. I.: Optical Properties and Radiative Forcing of Southern African Biomass Burning Aerosol, Ph.D. thesis, 180 pp., Univ. of Washington, Seattle, 2006.

Magi, B. I., Fu, Q., Redemann, J., and Schmid, B.: Using aircraft measurements to estimate the magnitude and uncertainty of the shortwave direct radiative forcing of southern African biomass burning aerosol, J. Geophys. Res., 113, D05213, doi:10.1029/2007JD009258, 2008.

Magi, B. I., Ginoux, P. A., Ming, Y., and Ramaswamy, V.: Evaluation of tropical and extratropical Southern Hemisphere African aerosol properties simulated by a climate model, J. Geophys. Res., doi:10.1029/2008JD011128, in press, 2009.

Matichuk, R. I., Colarco, P. R., Smith, J. A., and Toon, O. B.: Modeling the transport and optical properties of smoke aerosols from African savanna fires during the Southern African Regional Science Initiative campaign (SAFARI 2000), J. Geophys. Res., 112, D08203, doi:10.1029/2006JD007528, 2007.

Meehl, G. A., Stocker,T. F., Collins, W. D., Friedlingstein, P., Gaye, A. T., Gregory, J. M., Kitoh, A., Knutti, R., Murphy, J. M., Noda, A., Raper, S. C. B., Watterson, I. G., Weaver, A. J., and Zhao, Z.-C.: Global Climate Projections, in: Climate Change 2007: The Physical Science Basis. Contribution of Working Group I to the Fourth Assessment Report of the Intergovernmental Panel on Climate Change, edited by: Solomon, S., Qin, D., Manning, M., Chen, Z., Marquis, M., Averyt, K. B., Tignor, M., and Miller, H. L., Cambridge University Press, Cambridge, UK and New York, NY, USA, 2007.

Piketh, S. J., Annegarn, H. J., and Tyson, P. D.: Lower tropospheric aerosol loadings over South Africa: the relative contribution of aeolian dust, industrial emissions, and biomass burning, J. Geophys. Res., 104(D1), 1597–1607, 1999.

Posfai, M., Simonics, R., Li, J., Hobbs, P. V., and Buseck, P. R.: Individual aerosol particles from biomass burning in southern Africa: 1. Compositions and size distributions of carbonaceous particles, J. Geophys. Res., 108(D13), 8483, doi:10.1029/2002JD002291, 2003.

Ruellan, S., Cachier, H., Gaudichet, A., Masclet, P., Lacaux, J.: Airborne aerosols over central Africa during the Experiment for Regional Sources and Sinks of Oxidants (EXPRESSO),

J. Geophys. Res., 104(D23), 30673–30690, 1999.

Seinfeld, J. H. and Pandis, S. N.: Atmospheric Chemistry and Physics: From Air Pollution to Climate Change, 2nd Ed., Wiley, New Jersey, 1203 pp., 2006.

Sinha, P., Hobbs, P. V., Yokelson, R. J., Bertschi, I. T., Blake, D. R., Simpson, I. J., Gao, S., Kirchstetter, T. W., and Novakov, T.: Emissions of trace gases and particles from savanna fires in southern Africa, J. Geophys. Res., 108(D13), 8487, doi:10.1029/2002JD002325, 2003.

Stier, P., Feichter, J., Kinne, S., Kloster, S., Vignati, E., Wilson, J., Ganzeveld, L., Tegen, I., Werner, M., Balkanski, Y., Schulz, M., Boucher, O., Minikin, A., and Petzold, A.: The aerosol-climate model ECHAM5-HAM, Atmos. Chem. Phys., 5, 1125–1156, 2005, http://www.atmos-chem-phys.net/5/1125/2005/.

Sun, H., Biedermann, L., and Bond, T. C.: Color of brown carbon: a model for ultraviolet and visible light absorption by organic carbon aerosol, Geophys. Res. Let., 34, L17813, doi:10.1029/2007GL029797, 2007.

Swap, R. J., Annegarn, H. J., Suttles, J. T., King, M. D., Platnick, S., Privette, J. L., and Scholes,R. J.: Africa burning: a thematic analysis of the Southern African Regional Science Initiative (SAFARI 2000), J. Geophys. Res., 108(D13), 8465, doi:10.1029/2003JD003747, 2003.

Tang, I. N. and Munkelwitz, H. R.: Water activities, densities, and refractive indices of aqueous sulfates and sodium nitrate droplets of atmospheric importance, J. Geophys. Res., 99(D9), 18801–18808, 1994.

Tripathi, B. D., Chaturvedi, S. S., and Tripathi, R. D.: Seasonal variation in ambient air concentration of nitrate and sulfate aerosols in a tropical city, Varanasi, Atmos. Env., 30(15), 2773–2778, 1996.

Turpin, B. J. and Lim, H. J.: Species contributions to $PM_{2.5}$ mass concentrations: revisiting common assumptions for estimating organic mass, Aerosol Sci. Tech., 35, 602–610, 2001.

White, W. H.: The Chemical Composition of Fine Particles, Visibility: Existing and Historical Conditions – Causes and Effects, edited by: Trijonis, J. C., US National Acid Precipitation Assessment Program, Washington D.C., 90–94, 1990.

Wild, M.: Short-wave and long-wave surface radiation budgets in GCMs: a review based on the IPCC-AR4/CMIP3 models, Tellus, 60A, 932–945, 2008.

Table 1. Characteristic properties of the extratropical and tropical Southern Hemisphere African aerosol measured during SAFARI-2000, which include the median values (and interquartile range, IQR) of aerosol optical depth (AOD), single scattering albedo (SSA), asymmetry parameter (ASY), relative humidity (RH), aerosol number concentration (N_1, N_2), coarse to fine particle volume ratio (C/F), and aerosol angstrom exponent (α).

	Extratropics		Tropics	
	Median	IQR	Median	IQR
AOD[a]	0.23	0.19–0.33	1.07	0.72–1.11
SSA[a]	0.89	0.87–0.91	0.83	0.83–0.84
ASY[a]	0.56	0.51–0.57	0.58	0.53–0.59
RH (%)	31	29–32	25	15–27
N_1 (cm^{-3})[b]	2904	1507–5441	4930	4527–5075
N_2 (cm^{-3})[c]	632	442–768	1326	986–1461
C/F (%)[d]	2.66	1.80–2.91	1.44	1.35–1.57
α[e]	1.76	1.68–1.87	1.85	1.77–1.87

[a] At a wavelength of 550 nm.

[b] For particles with diameters 0.003–1 µm.

[c] For particles with diameters 0.1–3 µm.

[d] Volume ratio of coarse mode particles (1–3 µm diameter) to fine mode particles (0.1–1 µm diameter).

[e] For extinction coefficient between 450 and 700 nm.

Table 2. Comparison of median aerosol mass concentrations (µg/m^3) and interquartile range (IQR) reported by Gao et al. (2003), G2003, and Kirchstetter et al. (2003), K2003, versus those reported by Eatough et al. (2003), E2003, for samples representative of Southern Hemisphere African (a) extratropics and (b) tropics.

	Data source:	G2003 or K2003		E2003	
	Species	Median	IQR	Median	IQR
(a)	PM$_{2.5}$	22.7	16.6–36.9	14.0	8.7–27.4
	OC	4.2	3.4–5.1	3.5	3.4–9.3
	BC	0.8	0.7–1.3	0.9	0.5–1.8
	SO$_4$	6.0	4.7–12.0	4.0	1.8–6.5
	NO$_3$	0.4	0.3–0.5	0.2	0.1–0.4
(b)	PM$_{2.5}$	19.1	14.1–20.1	43.7	31.1–63.6
	OC	15.0	10.5–20.3	20.2	14.6–26.4
	BC	3.8	2.6–5.1	1.6	1.2–1.8
	SO$_4$	1.0	0.9–1.1	7.7	5.7–8.1
	NO$_3$	0.8	0.5–1.0	2.8	2.0–5.6

Table 3. Results of simultaneous filter samples showing aerosol mass concentrations (μg/m^3) determined using one of the three flow meters on the research aircraft.

Flow meter ID	$PM_{2.5}$	NO_3	SO_4	OC	BC
Test 1					
Flow 1	13.4	0.7	0.8	5.0	2.1
Flow 2	46.6	3.1	3.7	16.8	4.3
Test 2					
Flow 2	23.0	0.9	2.4	7.5	1.5
Flow 3	39.6	1.9	5.8	16.5	3.5

Table 4. Comparison of median aerosol mass concentrations (µg/m^3) and interquartile range (IQR) reported by Gao et al. (2003), G2003, and Kirchstetter et al. (2003), K2003, versus those reported by Eatough et al. (2003), E2003, for samples representative of Southern Hemisphere African (a) extratropics and (b) tropics after we applied corrections based on Table 3.

	Data source:	G2003 or K2003		E2003	
	Species	Median	IQR	Median	IQR
(a)	$PM_{2.5}$	11.5	8.2–16.7	14.0	8.7–27.4
	OC	4.2	3.4–5.1	3.5	3.4–9.3
	BC	0.8	0.7–1.3	0.9	0.5–1.8
	SO_4	2.7	2.2–5.4	4.0	1.8–6.5
	NO_3	0.2	0.2–0.3	0.2	0.1–0.4
(b)	$PM_{2.5}$	48.3	41.2–66.1	43.7	31.1–63.6
	OC	16.5	11.5–19.5	23.2	17.1–36.2
	BC	4.2	2.7–5.5	1.8	1.4–1.8
	SO_4	3.3	3.0–3.6	7.7	5.7–8.1
	NO_3	2.4	1.5–3.0	2.8	2.0–5.6

Table 5. Mass concentrations (µg/m^3) of $PM_{2.5}$ and species contributing to $PM_{2.5}$ (OC, BC, SO_4, NO_3, and SVOC) samples representative of the extratropics and the tropics of Southern Hemisphere Africa. Statistics are presented as median and interquartile range (IQR). OM is calculated as 1.4×OC in the extratropics, and 2.1×OC in the tropics (see discussion in text).

	Extratropics		Tropics	
Species	Median	IQR	Median	IQR
$PM_{2.5}$	11.5	8.1–19.8	47.5	38.3–66.5
OC	3.9	3.4–5.3	17.1	12.0–22.6
BC	0.9	0.6–1.3	3.4	1.8–4.5
SO_4	3.7	2.2–6.1	3.4	3.1–3.8
NO_3	0.2	0.1–0.3	2.6	1.5–3.0
SVOC	5.6	3.2–8.7	5.7	5.7–50.5
OM	5.3	4.6–7.2	36.0	25.3–47.7

Table 6. The mass scattering cross sections for organic carbon (MSC_{OC}), black carbon (MSC_{BC}), sulfate (MSC_{SO_4}), and nitrate (MSC_{NO_3}) and the mass absorption cross sections for organic carbon (MAC_{OC}) and black carbon (MAC_{BC}), as derived from measurements and from Mie theory. The units are m^2/g and MSC and MAC are at a wavelength of 550 nm.

	Measurements	Mie
MSC_{OC}	3.9±0.6	3.7
MSC_{BC}	1.6±0.2	1.5
MSC_{SO_4}	0.6±0.8	0.3
MSC_{NO_3}	0.6±0.8	0.4
MAC_{OC}	0.7±0.6	0.6
MAC_{BC}	8.2±1.1	7.9

Table 7. Aerosol characteristics used to calculate Mie mass scattering cross section and mass absorption cross section. The geometric mean diameter (D_g) and geometric standard deviation (σ_g) describe the lognormal aerosol size distribution. The real and imaginary refractive indices (m_{real} and m_{imag}) are at a wavelength of 550 nm.

Species	D_g (nm)	σ_g	Density (g/cm^3)	m_{real}	m_{imag}
OC	150	2.0	1.40	1.50	0.03
BC	35	1.8	1.35	1.85	0.72
$(NH_4)_2SO_4$	50	1.5	1.80	1.53	10^{-7}
NH_4NO_3	50	1.5	1.80	1.56	10^{-9}

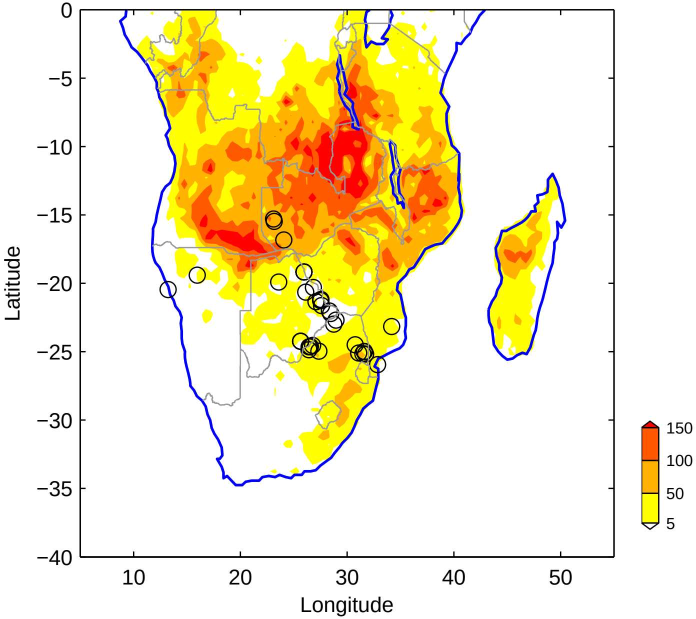

Fig. 1. Locations of filter samples collected during the SAFARI-2000 field campaign (black circles). Colors are mean (2001–2007) August and September fire counts derived from Moderate Resolution Imaging Spectroradiometer (MODIS) measurements (Collection 5) in units of fires per half degree gridcell.

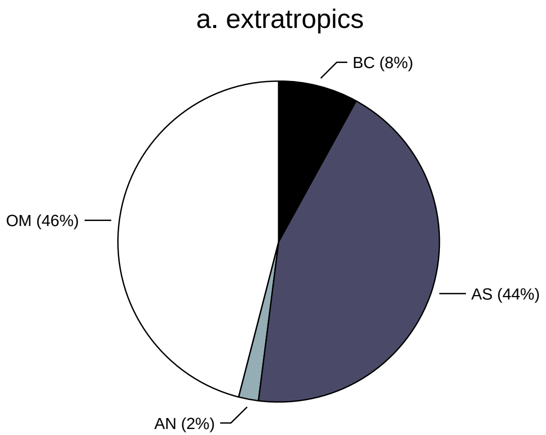

Fig. 2. Apportionment of $PM_{2.5}$ aerosol mass concentrations for **(a)** extratropical southern Africa and **(b)** tropical southern Africa. Shown are the median percent contributions of organic matter (OM), black carbon (BC), ammonium nitrate (AN), and ammonium sulfate (AS).

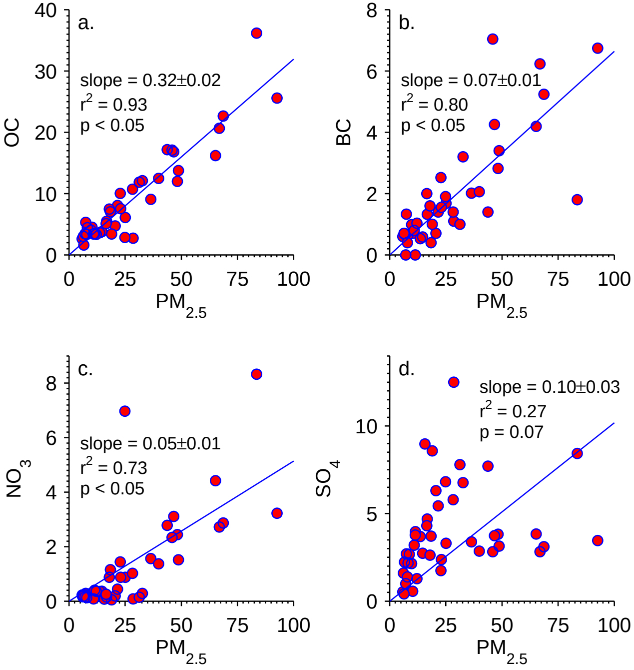

Fig. 3. Correlation of mass concentrations (μg/m^3) of **(a)** organic carbon (OC), **(b)** black carbon (BC), **(c)** nitrate ions (NO_3), and **(d)** sulfate ions (SO_4) with particulate matter with diameters less than 2.5 μm ($PM_{2.5}$). Listed in the figures are the slopes and 95% confidence interval of the linear regression, the correlation coefficients (r^2), and the p-values (p) of the correlation.

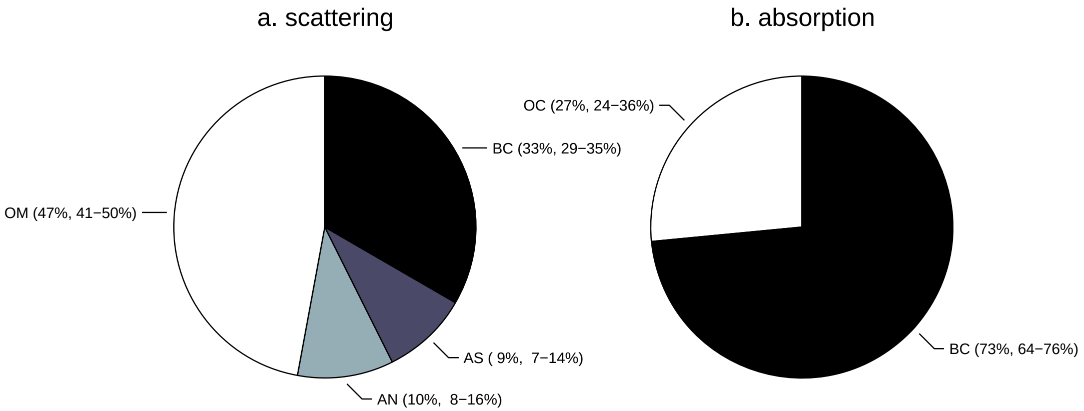

Fig. 4. Apportionment of **(a)** scattering and **(b)** absorption at a wavelength of 550 nm in extratropical southern Africa. Shown are the median percent contributions (with the interquartile range) of organic matter (OM), black carbon (BC), ammonium nitrate (AN), and ammonium sulfate (AS).

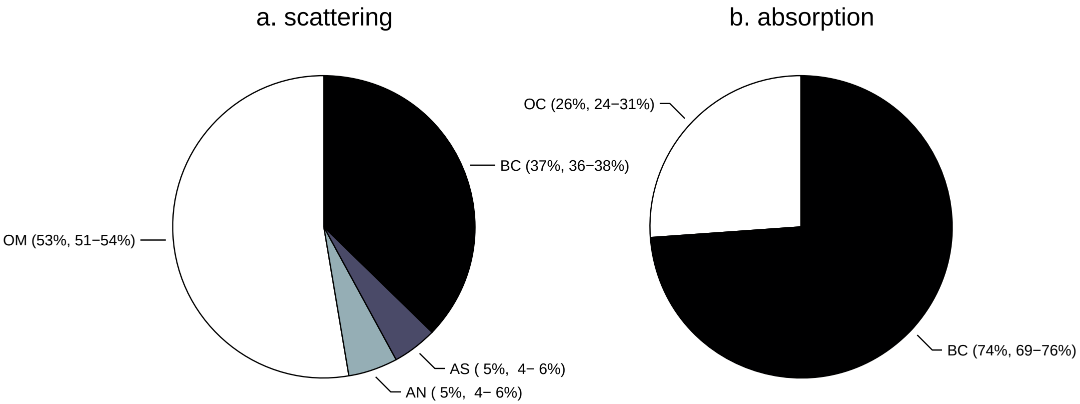

Fig. 5. Apportionment of **(a)** scattering and **(b)** absorption at a wavelength of 550 nm in tropical southern Africa. Shown are the median percent contributions (with the interquartile range) of organic matter (OM), black carbon (BC), ammonium nitrate (AN), and ammonium sulfate (AS).